High-Index Facets

DOI: 10.1002/anie.201007771

Anatase TiO_2 Crystals with Exposed High-Index Facets**

Hai Bo Jiang, Qian Cuan, Ci Zhang Wen, Jun Xing, Di Wu, Xue-Qing Gong, Chunzhong Li, and Hua Gui Yang**

Inorganic functional materials with tailor-made crystal facets have attracted great research interest owing to their applications in catalysis, sensors, batteries, and environmental remediation.[1–6] Unfortunately, the surfaces with high reactivity usually diminish rapidly during the crystal growth process as a result of the minimization of surface energy. Thus, increasing the percentage of known highly reactive surfaces or creating new favorable surfaces is highly desirable. Crystalline titanium dioxide (TiO_2) in the anatase phase is one of the most important semiconducting metal oxides, owing to its many promising energy and environmental applications.[7–9] Conventionally, anatase TiO_2 crystals are dominated by the thermodynamically stable {101} facets (ca. 94 percent, according to the Wulff construction) and a minority of {001} facets.[10] Recently, we developed a new strategy to synthesize anatase TiO_2 crystals with a large percentage of highly reactive {001} facets using fluorine-containing compounds, such as hydrofluoric acid, as capping agents, which made {001} energetically preferable to {101}.[4] Gas-phase reactions with rapid heating and quenching were also reported recently to generate {001}-faceted decahedral anatase TiO_2 crystals.[11] Most recently, photocatalytically active {100} facets of anatase TiO_2 crystals were synthesized using solid sodium titanates as the titanium source under hydrothermal conditions.[12] However, all these breakthroughs contribute to the increase of the percentage of known low-index {001} or {100} facets only, which are the basic crystal surfaces in the Wulff construction model of anatase in a thermodynamically stable state and have been evidenced theoretically and experimentally.[13]

Because they usually have unique surface atomic structures, such as a high density of atomic steps, dangling bonds, kinks, and ledges, that can act as active sites, high-index planes of anatase may have the capability to be used in clean-energy and environmental applications. Unfortunately, owing to the high surface energies, which can lead to the elimination of high-index crystal planes, it is still an open challenge to synthesize tailor-made anatase TiO_2 crystals bounded by high-index facets. Herein we report a facile process to prepare well-defined anatase TiO_2 crystals with predominantly exposed high-index {105} facets, which have never been realized experimentally before.

The anatase TiO_2 crystals with exposed high-index {105} facets were prepared by a modified high-temperature gas-phase oxidation route using titanium tetrachloride ($TiCl_4$) as the Ti source.[11] A schematic reaction apparatus is given in Figure S1 in the Supporting Information. A straight static furnace pipe and a thin spiral tube were used as reactor and reactant feeder, respectively. In a typical experiment, the vapor-phase $TiCl_4$ was liberated by bubbling oxygen ($0.2\ L\,min^{-1}$) into $TiCl_4$ liquid at 98 °C and then passed through the furnace pipe at a temperature of 1000 °C. The experimental process was shown to be quite robust, and the reproducible synthesis of the anatase TiO_2 crystals with exposed high-index {105} facets was also confirmed. Moreover, key synthesis conditions such as concentration of titanium precursor, reaction temperature, and oxygen flow were also explored extensively. In all experiments, the final white products were collected downstream by a bag filter and washed with deionized water three times to remove the adsorbed chlorine-containing species on the surface. Gram-scale production can be easily achieved if a furnace pipe with a diameter of about 5 cm is used (Figure S2 in the Supporting Information for digital camera images of the final white powder). Figure 1 shows the X-ray diffraction (XRD) pattern of the as-synthesized TiO_2 crystals with exposed high-index {105} facets. All the main diffraction peaks can be indexed to the anatase crystal phase (space group $I4_1/amd$, JCPDS No. 21-1272), and only a very small amount of rutile impurity can be detected. Moreover, the peak indexed to {105} facets exhibits a higher intensity than in the calculated diffraction pattern of bulk anatase, which indicates that more {105} facets have been exposed (the corresponding peak has been marked with an asterisk (*) in Figure 1). Scanning electron microscopy (SEM) images in Figure 2 a–c show that the synthesized

[*] Dr. H. B. Jiang, C. Z. Wen, J. Xing, Prof. Dr. C. Li, Prof. Dr. H. G. Yang
Key Laboratory for Ultrafine Materials of Ministry of Education
School of Materials Science and Engineering
East China University of Science and Technology
Shanghai, 200237 (China)
Fax: (+86) 21-6425-2127
E-mail: czli@ecust.edu.cn
hgyang@ecust.edu.cn
Q. Cuan, D. Wu, Prof. Dr. X. Q. Gong
Labs for Advanced Materials
Research Institute of Industrial Catalysis
East China University of Science and Technology
Shanghai, 200237 (China)

[**] This work was financially supported by the Scientific Research Foundation of East China University of Science and Technology (YD0142125), the Pujiang Talents Programme and Major Basic Research Programme of Science and Technology Commission of Shanghai Municipality (09J1402800, 10JC1403200), the Shuguang Talents Programme of Education Commission of Shanghai Municipality (09SG27), the National Natural Science Foundation of China (20973059, 91022023, 21076076, 20925621, 20703017), the Fundamental Research Funds for the Central Universities (WJ0913001), and the Program for New Century Excellent Talents in University (NCET-09-0347).

Supporting information for this article is available on the WWW under http://dx.doi.org/10.1002/anie.201007771.

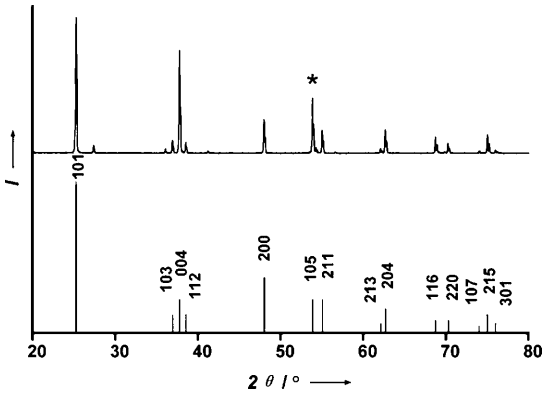

Figure 1. XRD pattern of the as-obtained anatase TiO_2 crystals dominated by high-index {105} facets. *: diffraction angle of (105) crystal planes.

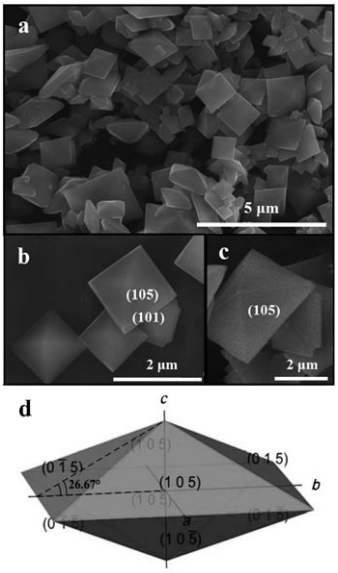

Figure 2. a–c) SEM images and d) schematic shape of the as-obtained anatase TiO_2 crystals dominated by high-index {105} facets.

anatase TiO_2 crystals display bipyramidal morphology with an average length of 2.42 μm (Figure S3 for the size distribution of these TiO_2 crystals). The 3D schematic shape of a typical anatase TiO_2 bipyramidal crystal with only high-index {105} facets exposed is shown in Figure 2d. Statistically, the average interfacial angle indicated in Figure 2d is 26.67°, which is close to that of {105} and {001} facets. The surfaces of all the crystals are very smooth, and some minority {101} facets can also be found occasionally, as indicated in Figure 2b and Figure S4 in the Supporting Information. According to the symmetries of anatase TiO_2, it can be concluded that the eight triangular surfaces in the bipyramidal crystals must be the high-index (105) facets. A transmission electron microscopy (TEM) image of a free-standing anatase TiO_2 bipyramidal crystal and its corresponding selected-area electron diffraction (SAED) pattern (Figure 3a,b) demonstrate the single-crystal characteristics. The high-magnification TEM image in Figure 3c clearly shows the (200) and (020) atomic planes

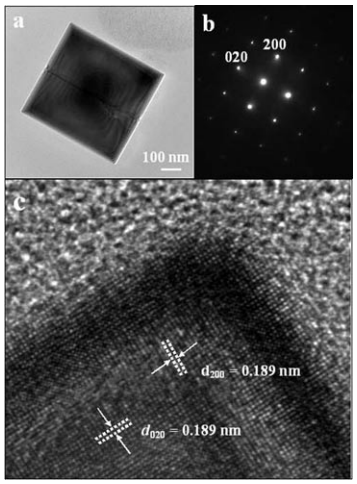

Figure 3. a) TEM image, b) SAED pattern, and c) high-resolution TEM image of a bipyramidal anatase TiO_2 crystal dominated by high-index {105} facets.

with a lattice spacing of 0.189 nm. It should be noted that both the SAED pattern and the high-magnification TEM image were indexed along the [001] crystallographic direction of anatase TiO_2.

Further experiments were carried out to investigate the effects of synthesis conditions such as reaction temperature, oxygen flow, or concentration of the titanium precursor. When the reaction temperature in the furnace pipe was lowered to 700–800 °C while all other reaction conditions were kept unchanged, polycrystalline TiO_2 particles were prepared, which was evidenced by XRD and TEM/SAED analysis (Figures S5a and S6 in the Supporting Information). However, if the reaction temperature was set to 900 °C, anatase TiO_2 single crystals bounded by {105} facets were generated, and the yield of the well-formed crystals was similar to that of the products prepared at 1000 °C (Figures S5a and S6 in the Supporting Information). Interestingly, oxygen flow, which can change the concentration of titanium precursor and the residence time of reactants in the reaction region, was also found to have a significant effect on the formation of highly reactive {105} facets. The high oxygen flow (0.5 $L\,min^{-1}$) can lead to the formation of anatase TiO_2 nanocrystals with irregular shape and broad particle size distribution, while low oxygen flow (0.2–0.4 $L\,min^{-1}$) can generate anatase crystals dominated by {105} facets (Figures S5b and S7 in the Supporting Information).

The formation of high-index anatase {105} facets might be due to the synergistic effects of thermodynamic and kinetic factors that control the crystal nucleation and subsequent growth. The co-adsorption of oxygen, chlorine, and other related species generated during the $TiCl_4$ oxidization process may lower the Gibbs free energy of {105} facets specifically and thus stabilize the typical atomic configuration on {105} facets. On the other hand, the large excess of oxygen during the reaction may also affect the growth kinetics of anatase TiO_2 crystals in our case; the concentration of Ti starting material and the Ti/O ratio in the reaction system are very low and some Ti starting material consuming crystal facets such as

{101} or {103} can be effectively prevented. X-ray photoelectron spectra (XPS) of Cl 2p, Ti 2p, and O 1s for the anatase TiO_2 crystals dominated by high-index {105} facets are shown in Figure S8 in the Supporting Information. The oxidation state of the Ti in the products (Ti 2p3/2, binding energy 458.5 eV; Ti 2p1/2, binding energy 464.2 eV) is close to that in bulk anatase TiO_2.[14] Furthermore, Cl 2p exhibits two peaks at around 198.1 and 199.8 eV, which can be attributed to the typical surface Ti–Cl species.[15] The area of the Cl 2p peak diminished significantly after the products were washed by deionized water several times.

More importantly, in order to obtain the intermediate products which might give important clues for the growth mechanism of the high-index {105} facets, a copper-based cool-water tube was put into the central part of the furnace pipe to quench the temperature of the growing anatase TiO_2 single crystals attached to the surface (Figure S9 in the Supporting Information for structural information on the cool water tube), and some early products were successfully collected. As shown in Figure 4 a–e, all anatase TiO_2 crystals are bounded by well-formed {101} and {001} facets, and TEM, HRTEM, and SAED results along the crystallographic [010] direction (Figure S10 in the Supporting Information) also illustrate the growing high-index facets besides these well-formed {101} and {001} facets on the intermediate products. Interestingly, some crystalline "tips" showing different morphologies can be observed on the central region of the two parallel {001} facets (Figure 4 a, b), which might be deemed as the "embryo" of the high-index facets. Furthermore, as judged from the external shape of these anatase TiO_2 single crystals (Figure 4 e), facets with even higher indices were observed. These facets can be indexed as {107}, because the average interfacial angle is 150.60°, which is close to the theoretical value of 151.52°. Considering that all these high-index facets such as {105} and {107} were observed on well-faceted anatase TiO_2 single crystals, we may expect that the crystal growth should follow a two-stage growth mechanism. That is, well-faceted anatase TiO_2 single crystals with a highly truncated morphology were formed initially, which is consistent with the previous report.[11] Then, according to the principle of lattice matching for gas-phase epitaxial processes, high-index facets of anatase TiO_2 start to appear on the existing {001} facets. It should be noted that this epitaxial process only involved one type of TiO_2 component, and the crystallographic structure of the anatase phase was also maintained. These structural similarities can make the anatase TiO_2 grow along the [001] direction easily, since no lattice strain exists in the interfacial region and well-faceted crystals can thus develop. On the basis of these observations, a plausible two-stage growth mechanism of anatase TiO_2 with high-index facets is proposed, as illustrated in Figure 4 f. These findings may also help us to understand the different stages of crystal growth from thermodynamically unstable high-index surfaces to stable low-index surfaces and pave the way for the fabrication of some other unusual facets as well.

To understand surface structure and catalytic activity of {105} facets of anatase TiO_2, calculations were carried out using first-principles density functional theory (DFT). There are three possible structures of stoichiometric (105) surfaces

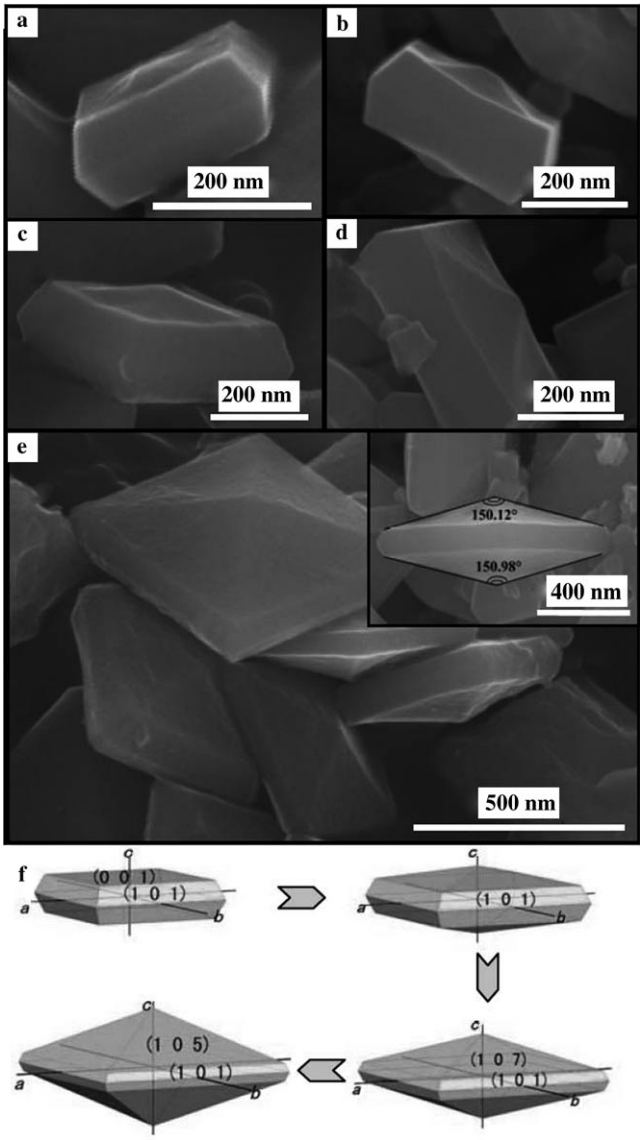

Figure 4. a–e) SEM images of typical underdeveloped anatase TiO_2 single crystals deposited on the low-temperature copper surface exposed in the reaction region, and f) a schematic depiction of the two-stage growth process of anatase TiO_2 with exposed high-index {105} facets.

of anatase TiO_2 (Figure S11 in the Supporting Information), and they all expose the (001) facet and (100)-type step edges; the only difference is the relative ratio of {001} and {100} facets and the orientation of these facets at the (105) surfaces. The total-energy calculations show that the first structure gives the best stability, which indicates that {105} facets are most possibly exposed by such a structure. The exact surface energy of the (105) surface with the first structure shown in Figure S11 in the Supporting Information was estimated to be 0.84 $J\,m^{-2}$. This value is lower than that of unreconstructed anatase TiO_2 (001) (ca. 1.0 $J\,m^{-2}$) but is significantly higher than that of anatase TiO_2 (101) (ca. 0.5 $J\,m^{-2}$). Furthermore, from the calculated electronic density of states (Figure S12 in the Supporting Information), we can clearly see that the oxygen and titanium at the step edge (blue arrows) contribute

significantly to the edges of valence and conduction bands, respectively.

We then also used this (105) surface for the study of its activity. Two side views of the adsorption mode of H_2O on the anatase TiO_2 (105) surface are illustrated in Figure 5. It was found that H_2O can only adsorb along the step edges dissociatively, while it is unable to stay at the flat facet. The adsorption energy was estimated to be 1.03 eV under the local coverage of 1/2 (with respect to the edge Ti or O).[1,16] From these results, it can be predicted that the {105} facets should have the capability to cleave water photocatalytically; they should perform better than pure {101} facets but not as well as pure {001} facets. Interestingly, the as-prepared anatase TiO_2 single crystals with exposed high-index {105} facets demonstrate the capability to cleave water to generate hydrogen gas, which was also confirmed experimentally. As shown in Figure S13 in the Supporting Information, the volume of hydrogen generated is proportional to the light irradiation time (0.65 mL in 2 h), and the evolution rate is lower than that of the anatase TiO_2 single crystals with exposed {001} facets,[11] which is consistent with the theoretical predictions.

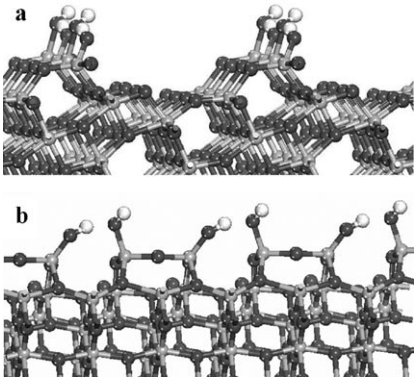

Figure 5. Calculated structures (a, b: two side views) of H_2O molecules at the anatase TiO_2 (105) surface. H white, O dark gray, Ti gray.

In conclusion, we have successfully synthesized anatase TiO_2 with high-index {105} facets by a simple gas-phase route for the first time. The products possess well-faceted surfaces and may have promising potential applications in renewable clean energy applications and environmental remediation owing to the unique stepped atomic configuration on the high-index {105} facets. Furthermore, the production method developed herein is very robust and can be scaled up easily, which may pave the way for the large-scale production of anatase TiO_2 crystals with exposed high-index {105} facets.

Experimental Section

The anatase TiO_2 crystals bounded by high-index {105} facets were prepared by a high-temperature gas-phase oxidation route using titanium tetrachloride ($TiCl_4$) as Ti source. A schematic reaction apparatus is given in Figure S1 in the Supporting Information. A straight static furnace pipe and a thin spiral tube were used as reactor and reactant feeder, respectively. In a typical experiment, the vapor-phase $TiCl_4$ was liberated by bubbling oxygen (0.2 L min^{-1}) into $TiCl_4$ liquid at 98 °C. The gas-phase mixture was then passed through the furnace pipe at a temperature of 1000 °C. The final white products were collected downstream by a bag filter and washed with deionized water three times to remove the adsorbed chlorine-containing species on the surface.

Crystallographic information of high-index anatase TiO_2 single crystals was obtained by X-ray diffraction (XRD, Bruker D8 Advanced Diffractometer, $Cu_{K\alpha}$ radiation, 40 kV). The morphology and structure of the samples were characterized by transmission electron microscopy and selected area electron diffraction (TEM/SAED, JEOL JEM-2010F) and by field-emission scanning electron microscopy (FESEM, HITACHI S4800). Chemical compositions and the bonding states of anatase TiO_2 single crystals were analyzed using X-ray photoelectron spectroscopy (XPS, Thermo ESCALAB 250, Al Kα exciting radiation). XPS spectra of Cl 2p, Ti 2p, and O 1s were measured with a constant analyzer-pass energy of 20.0 eV. All binding energies were referenced to the C 1s peak (284.8 eV) arising from surface hydrocarbons (or possible adventitious hydrocarbons). Prior peak deconvolution, X-ray satellites, and inelastic background (Shirley-type) were subtracted for all spectra.

The as-obtained TiO_2 product was loaded with 1 wt% Pt and calcinated at 350 °C for 2 h. The treated powder (50 mg) was then dispersed in aqueous solution (100 mL) containing 10 vol% methanol. A 300 W Xe lamp was used as light source. The amount of H_2 released was determined using gas chromatography (TECHCOMP, 7890II). To confirm its photocatalytic activity, anatase TiO_2 with exposed {001} facets was prepared according to the literature[4] and applied as a benchmarking material for hydrogen-evolution testing.

Received: December 10, 2010
Revised: January 17, 2011
Published online: March 17, 2011

Keywords: crystal engineering · high-index facets · nanostructures · solid-state structures · titanium dioxide

[1] A. Vittadini, A. Selloni, F. P. Rotzinger, M. Grätzel, *Phys. Rev. Lett.* **1998**, *81*, 2954 – 2957.
[2] A. Vittadini, M. Casarin, A. Selloni, *Theor. Chem. Acc.* **2007**, *117*, 663 – 671.
[3] M. Lazzeri, A. Selloni, *Phys. Rev. Lett.* **2001**, *87*, 266105.
[4] H. G. Yang, C. H. Sun, S. Z. Qiao, J. Zou, G. Liu, S. C. Smith, H. M. Cheng, G. Q. Lu, *Nature* **2008**, *453*, 638 – 641.
[5] a) H. G. Yang, G. Liu, S. Z. Qiao, C. H. Sun, Y. G. Jin, S. C. Smith, J. Zou, H. M. Cheng, G. Q. Lu, *J. Am. Chem. Soc.* **2009**, *131*, 4078 – 4083; b) S. Liu, J. Yu, M. Jaroniec, *J. Am. Chem. Soc.* **2010**, *132*, 11914 – 11916.
[6] a) X. Han, Q. Kuang, M. Jin, Z. Xie, L. Zheng, *J. Am. Chem. Soc.* **2009**, *131*, 3152 – 3153; b) N. Tian, Z. Zhou, S. Sun, Y. Ding, Z. L. Wang, *Science* **2007**, *316*, 732 – 735; c) X. Han, M. Jin, S. Xie, Q. Kuang, Z. Jiang, Y. Jiang, Z. Xie, L. S. Zheng, *Angew. Chem.* **2009**, *121*, 9344 – 9347; *Angew. Chem. Int. Ed.* **2009**, *48*, 9180 – 9183; d) J. S. Chen, T. Zhu, X. H. Yang, H. G. Yang, X. W. Lou, *J. Am. Chem. Soc.* **2010**, *132*, 13162 – 13164; e) X. Y. Ma, Z. G. Chen, S. B. Hartono, H. B. Jiang, J. Zou, S. Z. Qiao, H. G. Yang, *Chem. Commun.* **2010**, *46*, 6608 – 6610; f) C. H. Sun, X. H. Yang, J. S. Chen, Z. Li, X. W. Lou, C. Li, S. C. Smith, G. Q. Lu, H. G. Yang, *Chem. Commun.* **2010**, *46*, 6129 – 6131; g) D. Zhang, G. Li, H. Wang, K. M. Chan, J. C. Yu, *Cryst. Growth Des.* **2010**, *10*, 1130 – 1137; h) D. Zhang, G. Li, X. Yang, J. C. Yu, *Chem. Commun.* **2009**, 4381 – 4383; i) J. Yin, Z. Yu, F. Gao, J. Wang, H. Pang, Q. Lu, *Angew. Chem.* **2010**, *122*, 6472 – 6476; *Angew. Chem. Int. Ed.* **2010**, *49*, 6328 – 6332.
[7] A. Fujishima, K. Honda, *Nature* **1972**, *238*, 37 – 38.
[8] B. O'Regan, M. Grätzel, *Nature* **1991**, *353*, 737 – 740.
[9] M. Grätzel, *Nature* **2001**, *414*, 338 – 344.

[10] M. Lazzeri, A. Vittadini, A. Selloni, *Phys. Rev. B* **2001**, *63*, 155409.
[11] F. Amano, O. O. Prieto-Mahaney, Y. Terada, T. Yasumoto, T. Shibayama, B. Ohtani, *Chem. Mater.* **2009**, *21*, 2601 – 2603.
[12] J. Li, D. Xu, *Chem. Commun.* **2010**, *46*, 2301 – 2303.
[13] X. Q. Gong, A. Selloni, *J. Phys. Chem. B* **2005**, *109*, 19560 – 19562.
[14] X. W. Lou, H. C. Zeng, *J. Am. Chem. Soc.* **2003**, *125*, 2697 – 2704.
[15] P. Y. Shih, *J. Non-Cryst. Solids* **2003**, *315*, 211 – 218.
[16] C. Arrouvel, M. Digne, M. Breysse, H. Toulhoat, P. Raybaud, *J. Catal.* **2004**, *222*, 152 – 166.

